Computational Thermal Sciences, 2(3), 221–229 (2010)

RADIAL INJECTION OF A HOT FLUID INTO A COLD POROUS MEDIUM: THE EFFECTS OF LOCAL THERMAL NONEQUILIBRIUM

D. A. S. Rees[1,*] *& A. P. Bassom*[2]

[1]*Department of Mechanical Engineering, University of Bath, Bath BA2 7AY, United Kingdom*

[2]*School of Mathematics and Statistics, University of Western Australia, Crawley, WA 6009, Australia*

*Address all correspondence to D. A. S. Rees E-mail: D.A.S.Rees@bath.ac.uk

We consider the manner in which local thermal nonequilibrium effects influence the development of the thermal field when a hot fluid is injected radially into a cold porous medium. A purely forced convection situation is considered, and the evolving thermal fields depend on four non-dimensional parameters, including the Péclet number and the nondimensional interphase heat-transfer coefficient, H. In this primarily numerical study we find that local thermal equilibrium is always attained eventually, but after a time which depends strongly on the value of H. When the Péclet number is large a thermal shock wave is formed within the fluid phase which degrades slowly by imparting heat to the solid phase.

KEY WORDS: *forced convection,heat transfer, local thermal nonequilibrium, Keller box method*

1. INTRODUCTION

The aim of the present paper is to determine the different qualitative features of the evolution of the thermal field that may arise when a hot fluid is injected radially into a cold saturated porous medium under forced convective conditions. Should it be assumed that the fluid and solid phases are in local thermal equilibrium (by which is meant that, to a good approximation, heat is transferred between the phases sufficiently quickly that a single intrinsic temperature field may be adopted), then the evolving thermal field depends only on a suitably defined Péclet number. However, many situations exist in which it is necessary to adopt the local thermal nonequilibrium (LTNE) model, one example being the rapid ingress of hot fluid into low porosity relatively insulating porous medium, where heat is gained slowly by the solid phase. LTNE effects are modelled using the source/sink terms first introduced by Anzelius (1926) and Schumann (1929).

The present paper extends an earlier analysis by Rees et al. (2008) which considers the unidirectional infiltration of hot fluid into a cold porous medium. In that paper the velocity of the infiltrating fluid is constant, whereas the present paper has an infiltration speed which is inversely proportional to radius. Therefore we expect some qualitative differences between the two studies.

Direct injection of fluid into a porous medium has its most obvious application within the context of geothermal energy extraction, such as within a hot dry rock formation (Shook, 2001). The present configuration finds its application in the region close to an injection well; even more physical realism is likely to be found by considering the effect of an additional extraction well, and of multiple wells, but this is outside of the scope of the present work. Likewise, the effects of phase change, compressibility, temperature-dependent properties, buoyancy, and the presence of heterogeneities have been neglected for now. Further examples of this type of analysis may also be found in the references quoted by Rees et al. (2008).

1940–2503/10/$35.00

NOMENCLATURE

c	specific heat, $\mathrm{J\,kg^{-1}\,K^{-1}}$
h	interphase heat-transfer coefficient, $\mathrm{W\,m^{-3}\,K^{-1}}$
H	nondimensional form of h
k	conductivity, $\mathrm{W\,m^{-1}\,K^{-1}}$
LTE	local thermal equilibrium
LTNE	local thermal nonequilibrium
Pe	Péclet number
r	radial coordinate, m
r_0	inner radius, m
t	time, s
T	temperature, K
T_0, T_1	cold and hot temperatures, respectively, K
U_0	infiltration velocity at $r^* = r_0$
$\underline{v}$	fluid velocity vector
Greek symbols	
α	diffusivity ratio
γ	porosity-modified conductivity ratio
ε	porosity
η	similarity variable
θ	nondimensional fluid temperature
ρ	density, $\mathrm{kg\ m^{-3}}$
τ	scaled time
ζ	auxiliary variable
ϕ	nondimensional solid temperature
Subscripts/Superscripts	
f,s	fluid, solid
pm	porous medium
$*$	dimensional

We solve the full unsteady system of equations for the evolution of the temperature fields of the two phases using the Keller box method (Keller, 1978). These equations are parabolic in time and allow for spatial diffusion radially. Therefore we do not follow the studies of Shook (2001) and Stopa and Wojnarowski (2006), who employed hyperbolic approximations.

2. GOVERNING EQUATIONS

Suppose that a saturated porous medium occupies the region $r^* \geq r_0$, is homogeneous, and is isotropic. Cold fluid with temperature T_0 enters the medium with speed U_0 at $r^* = r_0$ and flows in the radial direction. At $t^* = 0$ the temperature of this injected fluid is raised suddenly to the new level, T_1. We assume that buoyancy forces are negligible and that forced convection conditions prevail. The evolution of the temperature fields of the fluid and solid phases is described by the Anzelius–Schumann model with the addition of thermal diffusion terms,

$$\varepsilon(\rho c)_{\mathrm{f}}\frac{\partial T_{\mathrm{f}}}{\partial t^*} + (\rho c)_{\mathrm{f}}\underline{v}^*\cdot\nabla T_{\mathrm{f}} = \varepsilon\nabla\cdot\left(k_{\mathrm{f}}\nabla T_{\mathrm{f}}\right) + h\left(T_{\mathrm{s}} - T_{\mathrm{f}}\right), \quad (1)$$

$$(1-\varepsilon)(\rho c)_{\mathrm{s}}\frac{\partial T_{\mathrm{s}}}{\partial t^*} = (1-\varepsilon)\nabla.(k_{\mathrm{s}}\nabla T_{\mathrm{s}}) + h(T_{\mathrm{f}} - T_{\mathrm{s}}), \quad (2)$$

where the background fluid velocity is given by $\underline{v}^* = (U_0/r_0)((r^*)^{-1}, 0, 0)$ in polar coordinates, i.e., the flow is in the radial direction. The value, h, which appears in Eqs. (1) and (2), is the interphase heat-transfer coefficient, the value of which is a function of the microscopic geometry of the medium, the conductivities of the phases, and the strength of the flow. Some values of h for stagnant two- and three-dimensional media of various types are given in Rees (2009, 2010).

As r_0 and U_0 are natural length and velocity scales, Eqs. (1) and (2) may be nondimensionalised using the transformations

$$r^* = r_0 r, \qquad \underline{v}^* = U_0\underline{v}, \qquad t^* = \frac{r_0^2(\rho C)_{\mathrm{pm}}}{k_{\mathrm{pm}}}t \quad (3)$$
$$(T_{\mathrm{f}}, T_{\mathrm{s}}) = T_0 + (T_1 - T_0)(\theta, \phi).$$

On assuming that the temperatures are dependent only upon r and t, the nondimensional equations become,

$$\left(\frac{\gamma+1}{\gamma+\alpha}\right)\frac{\partial\theta}{\partial t} + \frac{\mathrm{Pe}}{r}\frac{\partial\theta}{\partial r} = \frac{\partial^2\theta}{\partial r^2} + \frac{1}{r}\frac{\partial\theta}{\partial r} + H(\phi-\theta), \quad (4)$$

$$\alpha\left(\frac{\gamma+1}{\gamma+\alpha}\right)\frac{\partial\phi}{\partial t} = \frac{\partial^2\phi}{\partial r^2} + \frac{1}{r}\frac{\partial\phi}{\partial r} + H\gamma(\theta-\phi), \quad (5)$$

where the four nondimensional parameters are given by

$$H = \frac{hL^2}{\varepsilon k_f}, \qquad \gamma = \frac{\varepsilon k_f}{(1-\varepsilon)k_s}$$
$$\alpha = \frac{k_f}{(\rho C)_f}\frac{(\rho C)_s}{k_s} = \frac{\alpha_f}{\alpha_s}, \qquad \mathrm{Pe} = \frac{U_0 r_0 (\rho C)_f}{\varepsilon k_f}. \tag{6}$$

These are, respectively, an interphase heat-transfer coefficient, a diffusivity ratio, a porosity-scaled conductivity ratio, and a Péclet number based upon the fluid properties and the porosity.

We note, in passing, that when $H \gg 1$, which is the local thermal equilibrium (LTE) limit, it is possible to show that $\theta \sim \phi$, where

$$\frac{\partial \theta}{\partial t} + \frac{\mathrm{Pe}_{\mathrm{pm}}}{r}\frac{\partial \theta}{\partial r} = \frac{\partial^2 \theta}{\partial r^2} + \frac{1}{r}\frac{\partial \theta}{\partial r}, \tag{7}$$

and where

$$\mathrm{Pe}_{\mathrm{pm}} = \frac{\mathrm{Pe}\gamma}{1+\gamma} = \frac{U_0 r_0 (\rho C)_f}{k_{\mathrm{pm}}} \tag{8}$$

is a Péclet number based on the conductivity of the porous medium, $k_{\mathrm{pm}} = \varepsilon k_f + (1-\varepsilon)k_s$.

Equations (4) and (5) are to be solved subject to the initial condition that $\theta = \phi = 0$ for $t < 0$, and the boundary conditions, $\theta = 1$, $\partial\phi/\partial r = 0$ at $r = 1$, and $\theta, \phi \to 0$ as $r \to \infty$. As the mathematical problem consists of a sudden change in temperature of the fluid phase, it is natural to introduce the coordinate transformation

$$\eta = \frac{r-1}{2\sqrt{t}}, \qquad \tau = \sqrt{t}. \tag{9}$$

The governing equations now become

$$\left(\frac{\gamma+1}{\gamma+\alpha}\right)2\tau\frac{\partial \theta}{\partial \tau} = \frac{\partial^2 \theta}{\partial \eta^2} + \left[\left(\frac{\gamma+1}{\gamma+\alpha}\right)2\eta + \frac{2\tau(1-\mathrm{Pe})}{1+2\tau\eta}\right]\frac{\partial \theta}{\partial \eta} + 4\tau^2 H(\phi - \theta), \tag{10}$$

$$\alpha\left(\frac{\gamma+1}{\gamma+\alpha}\right)2\tau\frac{\partial \phi}{\partial \tau} = \frac{\partial^2 \phi}{\partial \eta^2} + \left[\alpha\left(\frac{\gamma+1}{\gamma+\alpha}\right)2\eta + \frac{2\tau}{1+2\tau\eta}\right]\frac{\partial \phi}{\partial \eta} + 4\tau^2 H\gamma(\theta - \phi). \tag{11}$$

The initial and boundary conditions remain unchanged, except that the initial conditions apply when $\tau = 0$, and the inner boundary conditions are imposed at $\eta = 0$.

Numerical solutions were undertaken using the Keller box method (Keller, 1978). This is a well-known technique which bears some relation to the Crank–Nicholson method, except that equations are usually reduced to first-order form, and it may also be applied to nonlinear systems. In general, we have used 0.025 as the spatial step as the maximum value of η-derivatives tended not to vary much with changes in the nondimensional parameters, although the maximum value for η increases with Pe. We used constant steps in $\log_{10}\tau$ in the range $10^{-4} \le \tau \le 10^3$ with an additional timestep at $\tau = 0$. The number of intervals used depended strongly on the values of the governing parameters. When either α or Pe is large, then rapid variations take place early in the evolution and these have to be resolved well. Similarly, when H is large, the thermal field within the solid phase adjusts rapidly toward the starting profile for the fluid phase.

3. RESULTS AND DISCUSSION

The governing equations contain four dimensionless parameters, and space does not allow a comprehensive presentation of our numerical results. However, we attempt to give a clear indication of the qualitative effect of varying each parameter in turn, and we also devote some space to determining the long-time fate of the temperature fields.

Figure 1 primarily shows how the isotherms for each phase vary with time, but it also serves a second purpose. The two columns of plots illustrate the evolution in different coordinate systems, namely, $(\eta, \log_{10}\tau)$ where η and τ are the computational coordinates, and (r, t), the physical coordinates. A direct comparison between the systems allows one to gain a rough idea of how variations in the physical coordinates appear when given isotherm plots in the computational coordinates. This is necessary because important features of the solution may be identified over many orders of magnitude of both r and t, and therefore Figs. 2–4 are presented in computational coordinates.

We concentrate first on the dependence of the thermal fields on the value of the Péclet number, as displayed in Fig. 1. In the (η, τ) coordinate system, at early times, the thermal field in the fluid phase is independent of time at leading order, as may be determined by taking a small τ expansion of the solutions of Eqs. (10) and (11). In addition, the early-time solution is also independent of the Péclet number, because the presence of the radial flow is felt first by the fluid phase at $O(\tau)$; see the second term in the coefficient multiplying $\partial\theta/\partial\eta$ in Eq. (10). On the other hand, the source/sink terms are of $O(\tau^2)$ in magnitude, meaning that the approach to LTNE begins later than the first observed influence of the radial flow, at least for moderate values of H and γ.

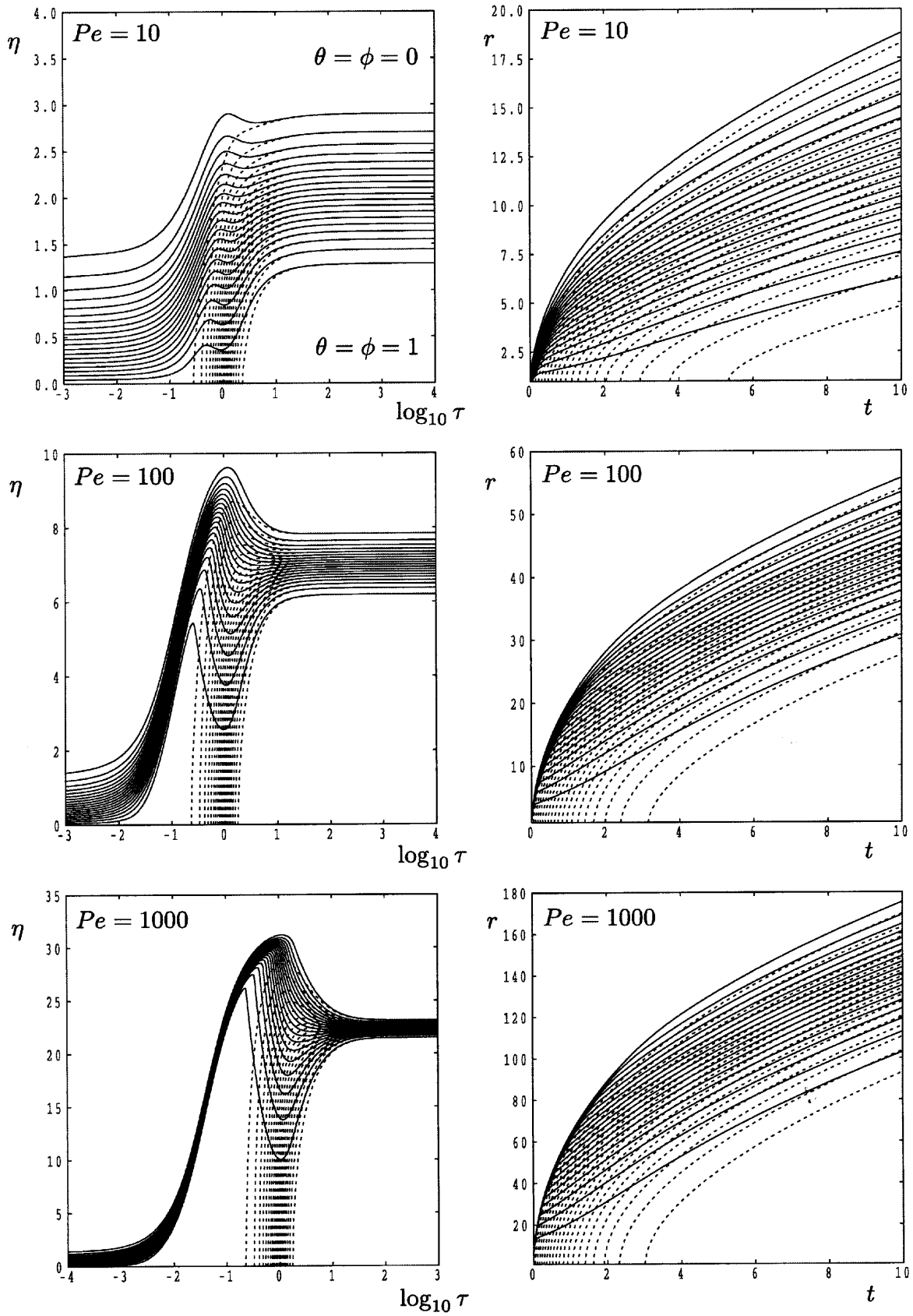

FIG. 1: Evolution with time of the temperature fields of the fluid (continuous lines) and solid (dashed lines) phases for three different values of the Péclet number, with $H = 1$, $\gamma = 1$, and $\alpha = 1$. Left-hand figures display isotherms in $(\eta, \log_{10}\tau)$ coordinates, while the right-hand figures use (r, t) coordinates.

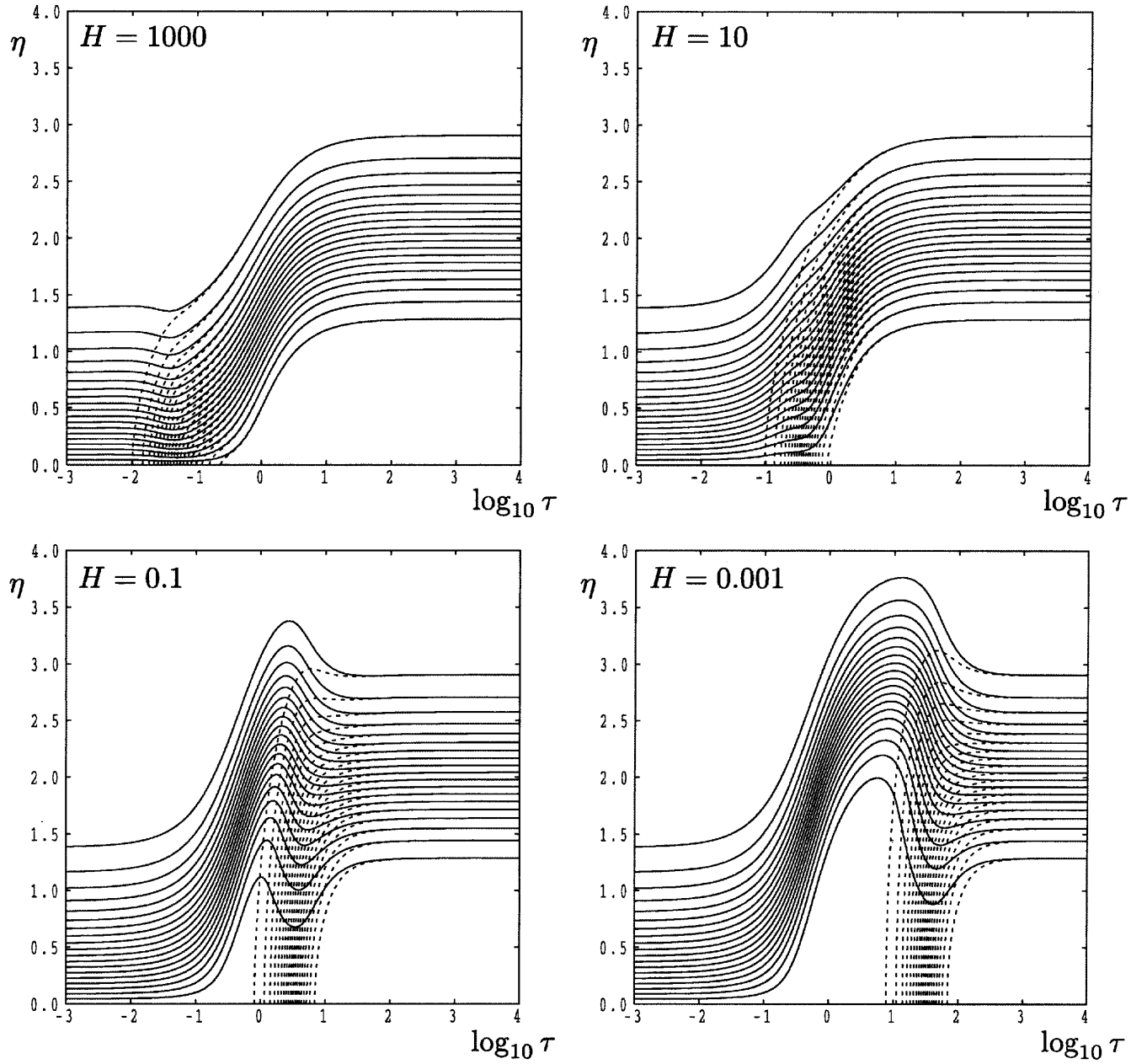

FIG. 2: Evolution with time of the temperature fields of the fluid (continuous lines) and solid (dashed lines) phases for four different values of H with Pe $= 10$, $\gamma = 1$, and $\alpha = 1$.

Given that H and γ take the same values in all three cases shown in Fig. 1, the left-hand frames show that the solid phase begins to heat up at the same time, independently of the value of Pe. However, the large time asymptotic location of the thermal front, in terms of η, recedes from the point of injection as the Péclet number increases. This is a direct consequence of the increasing magnitude of the background fluid velocity.

Once the solid phase begins to heat up, the fluid isotherms begin to backtrack to smaller values of η. This does not imply that conduction is taking place against the flow, for it is merely an artifact of the coordinate system, as may be seen in the accompanying right-hand frames which depict the location of the isotherms in terms of r and t.

Of most interest is the behaviour of the fluid isotherms as Pe increases, where, from the frames on the right, we see a thermal shock wave developing. This "shock" is a region of very rapid decay in the temperature of the fluid from 1 to 0. In this regard, this is the radial analogue of the thermal shock found in Rees et al. (2008) which also arises when the background fluid velocity is high. Once

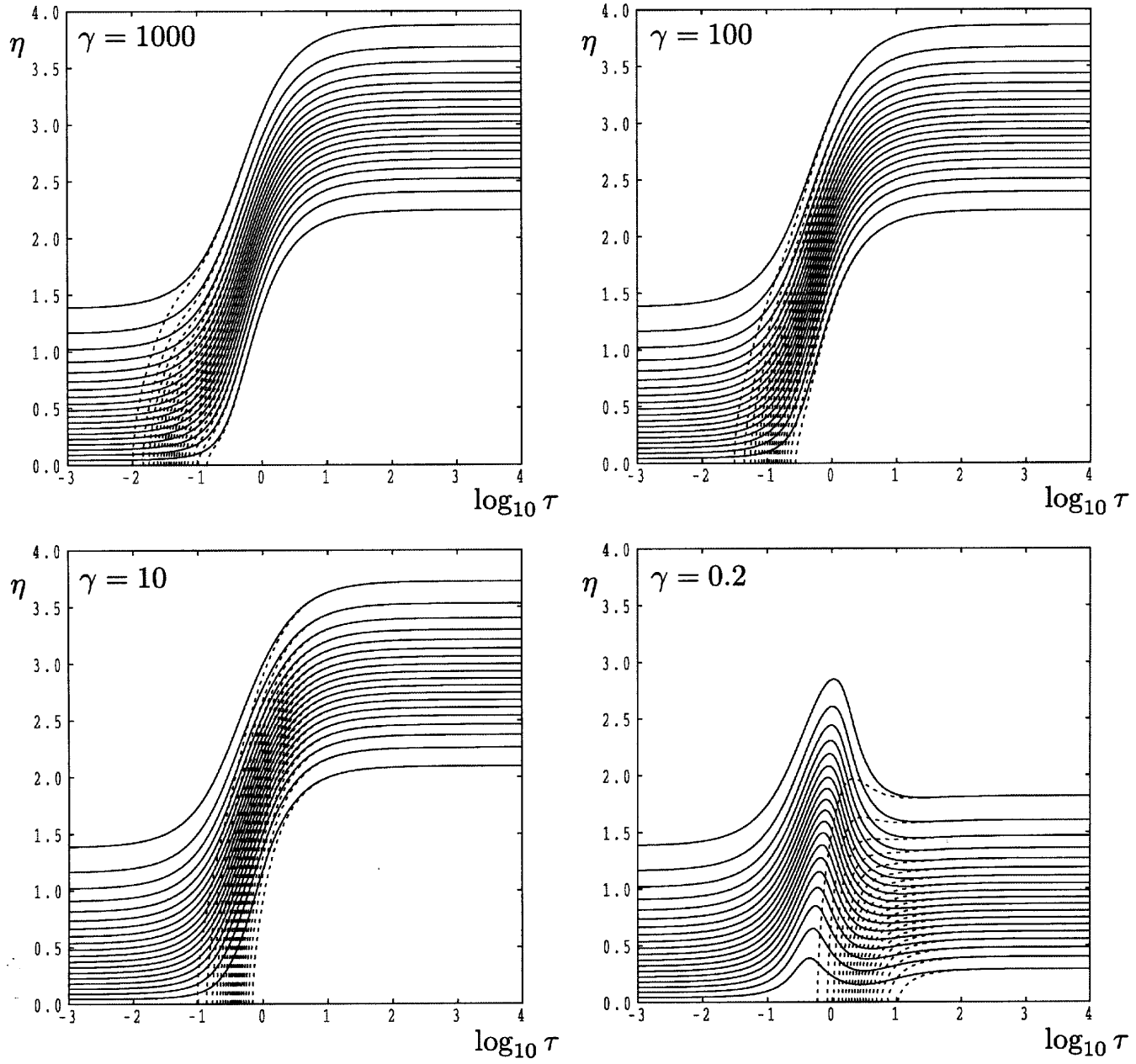

FIG. 3: Evolution with time of the temperature fields of the fluid (continuous lines) and solid (dashed lines) phases for four different values of γ with Pe $= 10$, $H = 1$, and $\alpha = 1$.

more, the strength of the shock decreases in time due to the fluid giving up heat to the solid phase; this is seen clearly in the right-hand frame for Pe $= 1000$.

At large times the two thermal fields settle down to identical τ-independent states when viewed within the (η, τ) system. In physical coordinates this means that there is a diffusing front with the centre travelling outwards with speed $t^{-1/2}$. In general, LTE is always achieved given sufficient time.

Figure 2 shows how different values of H affect the thermal fields. We note that both the early- and the late-time solutions are independent of the value of H. However, the time at which the solid phase begins to heat up depends very strongly on H. Rough indications based on the graphs suggest that this time is roughly proportional to $H^{-1/2}$, which is consistent with the fact that the source/sink terms in Eqs. (10) and (11) are multiplied by $\tau^2 H$.

Figure 3 depicts the manner in which different values of γ alter the thermal fields. Given that γ multiplies the source/sink term in Eq. (11) for ϕ, it clearly plays a similar role to that of H discussed above. The most obvious

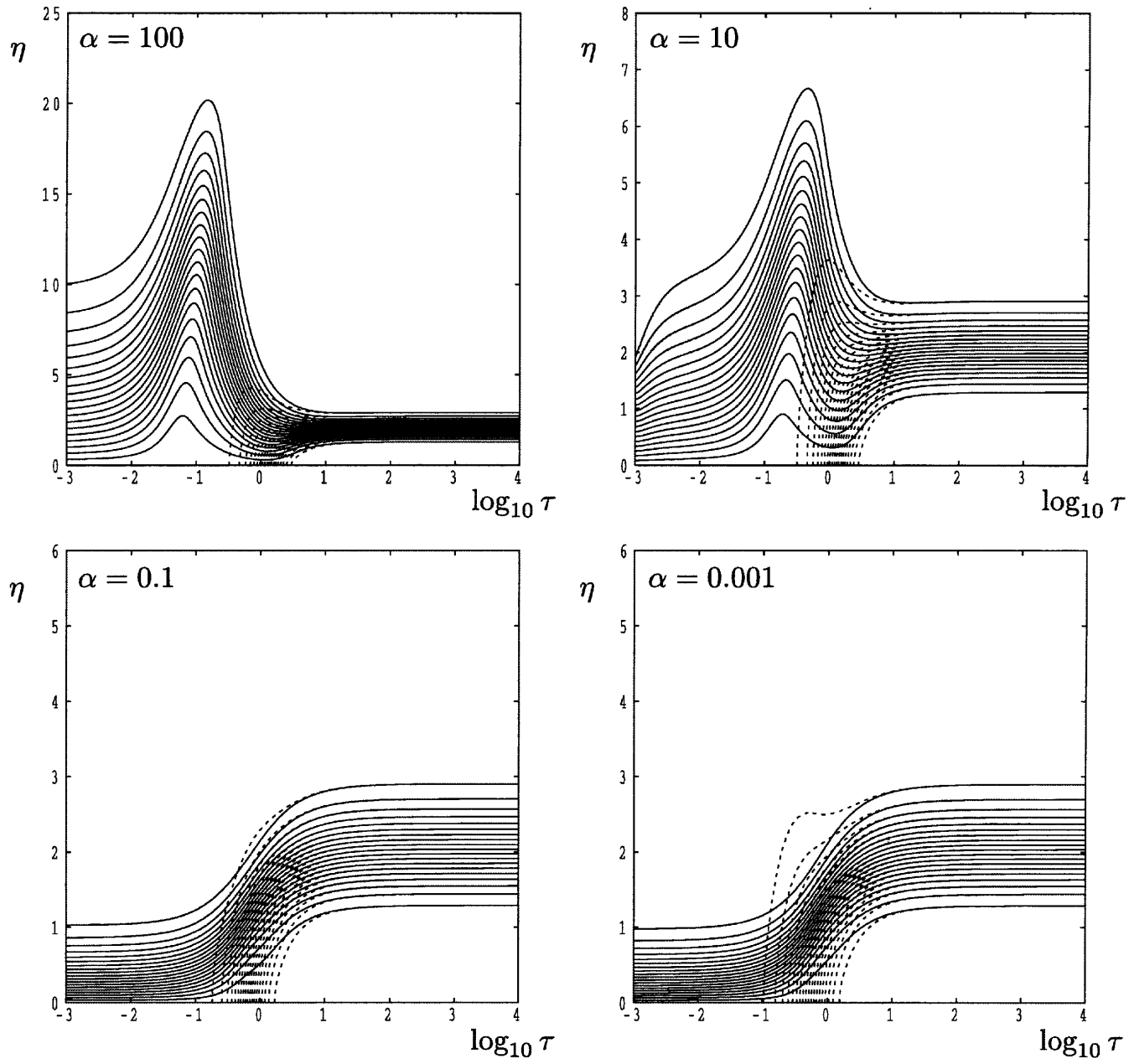

FIG. 4: Evolution with time of the temperature fields of the fluid (continuous lines) and solid (dashed lines) phases for four different values of α with Pe $= 10$, $H = 1$, and $\gamma = 1$.

effect of different values of γ is to vary the time at which the solid phase begins to heat up. This turns out to be proportional to $\gamma^{-1/2}$ for the same reason as mentioned in the previous paragraph. However, the large-τ solutions are now strongly dependent on the value of γ. Referring to Eq. (7), which applies when the phases are in LTE, the large-τ solution will clearly be dependent only on the value of $\mathrm{Pe_{pm}}$, which, given its definition in Eq. (8), means that the large-time solution depends on Pe and γ, but not on H or α. The solution for the smaller values of γ corresponds to LTE solutions for relatively small values of $\mathrm{Pe_{pm}}$, i.e., for slow rates of flow. The consequence of this is that the location of the large-time front will become closer to $\eta = 0$ as γ decreases.

The effects of different values of α are shown in Fig. 4. The early-time solution in the fluid phases is strongly dependent on α, which is explained mathematically below. From a physical point of view, large values of α corresponds to a relatively large thermal diffusivity of the fluid phase, which allows heat to conduct further from $\eta = 0$ ($r = 1$). The fluid isotherms then bend upward, which corresponds to the effect of the background flow,

but once the solid phase begins to heat, the temperature fields evolve to identical profiles with LTE. The time at which the solid begins to heat is weakly dependent on α. Of interest, however, is the behaviour of the solid-phase iostherms when α takes very low values. In such cases conduction within the solid phase takes place very rapidly and is able to overtake the finite propagation speed of the advective heat transport in the fluid phase. Once more, this rather unusual behaviour was seen to occur in the uniform infiltration problem studied by Rees et al. (2008).

4. LEADING ORDER ANALYSES AT EARLY AND LATE TIMES

At early times it is straightforward to show that that $\theta = O(1)$ and $\phi = O(\tau^2)$. A straightforward comparison of Eqs. (10) and (11) with Eqs. (2.9a and 2.9b) in Rees et al. (2008) shows that the leading-order, early time solutions are identical in the two cases. Specifically, we have

$$\theta \sim \operatorname{erfc}\zeta + O(\tau), \tag{12}$$

$$\phi \sim \frac{H\gamma(\gamma+\alpha)}{(1-\alpha)(\gamma+1)}\left[G(\zeta) - \frac{1}{\sqrt{\alpha}}G(\sqrt{\alpha}\zeta)\right]\tau^2 + O(\tau^3), \tag{13}$$

where

$$\zeta \equiv \left(\frac{\gamma+1}{\gamma+\alpha}\right)^{1/2}\eta \quad \text{and} \qquad G(\zeta) \equiv (2\zeta^2+1)\operatorname{erfc}\zeta - \frac{2}{\sqrt{\pi}}\zeta e^{-\zeta^2}. \tag{14}$$

The $O(\tau)$ term in Eq. (12) will be different from the one quoted in Rees et al. (2008), as will the $O(\tau^3)$ term in Eq. (13). This is because the speed of the background flow decreases radially; thus, we see that the thickness of the early-time boundary layer depends only on γ and α, and not on H or Pe.

At late times the numerical evidence suggests that the solutions are functions of η but not of τ, and that the thermal fields are in LTE. Therefore, we may analyze the τ-independent LTE version of Eqs. (10) and (11). It is straightforward to show that the large-τ solution is given by $\theta = \phi$ at leading order, where

$$\frac{\partial^2\theta}{\partial\eta^2} + \left(2\eta - \frac{\mathrm{Pe_{pm}}-1}{\eta}\right)\frac{\partial\theta}{\partial\eta} = 0, \tag{15}$$

and $\mathrm{Pe_{pm}}$ is defined in Eq. (8). This equation may be solved using an integrating factor approach to yield

$$\frac{\partial\theta}{\partial\eta} = \text{constant} \times \eta^{\mathrm{Pe_{pm}}-1}e^{-\eta^2}, \tag{16}$$

where the constant of integration may be found upon a second integration. After applying suitable boundary conditions we find that

$$\theta = \frac{\displaystyle\int_\eta^\infty \xi^{\mathrm{Pe_{pm}}-1}e^{-\xi^2}d\xi}{\displaystyle\int_0^\infty \xi^{\mathrm{Pe_{pm}}-1}e^{-\xi^2}d\xi}. \tag{17}$$

This may be transformed into the ratio of an upper incomplete gamma function and a gamma function:

$$\theta = \frac{\displaystyle\int_{\eta^2}^\infty \zeta^{\mathrm{Pe_{pm}}/2-1}e^{-\zeta}d\zeta}{\displaystyle\int_0^\infty \zeta^{\mathrm{Pe_{pm}}/2-1}e^{-\zeta}\,d\zeta} = \frac{\Gamma\left[\frac{1}{2}\mathrm{Pe_{pm}},\eta^2\right]}{\Gamma\left[\frac{1}{2}\mathrm{Pe_{pm}},0\right]}. \tag{18}$$

For positive integer values of $\mathrm{Pe_{pm}}$ which are multiples of 2, namely, when $\mathrm{Pe_{pm}} = 2n-2$, we may write this solution in the form

$$\theta = \sum_{i=1}^{n}\frac{\eta^{2i}e^{-\eta^2}}{(2i)!}. \tag{19}$$

However, we may gain useful information about the location of the diffusing thermal front by defining it as being where the temperature gradient is greatest. Therefore we may set the η-derivative of Eq. (16) to zero to obtain

$$\eta_{\mathrm{front}} = \sqrt{\mathrm{Pe_{pm}}-1}. \tag{20}$$

This formula is very accurate, as may be seen from the $\mathrm{Pe} = 100$ case in Fig. 1. Given that $\gamma = 1$, Eq. (8) yields $\mathrm{Pe_{pm}} = 50$, and thus Eq. (20) gives $\eta_{\mathrm{front}} = 7$. Figures 2–4 also confirm Eq. (20).

5. CONCLUSION

We have extended the numerical analysis of Rees et al. (2008) on the combined effect of LTNE and a uniform unidirectional infiltration of a hot fluid into a cold porous medium on the evolution of the respective temperature fields of the fluid and solid phases to the more realistic scenario of radial injection. Some of the qualitative features found in Rees et al. (2008) also arise for the radial injection problem, namely, the formation of a gradually decaying thermal shock at large values of the Péclet number, the effects of different values of H and γ on the time

at which the solid phase begins to heat up, the peculiar behaviour of the solid-phase isotherms when α is small, as shown in Fig. 4, and the eventual attainment of LTE at large times. The main qualitative difference arises at large times where the thickness of the advancing thermal front depends only on the value of $\mathrm{Pe}_{\mathrm{pm}} = \mathrm{Pe}\gamma/(1+\gamma)$. The work of Rees et al. (2008) shows that this thickness depends strongly on H, γ, and α.

There is no doubt that the effects of phase change, compressibility, temperature-dependent properties, buoyancy, and the presence of heterogeneities will alter our conclusions, possibility qualitatively, as will the presence of a production well, as this will alter the background flow field quite substantially. We hope to report on these matters at a later date.

REFERENCES

Anzelius, A., Über erwärmung vermittels durchströmender medien, *Zeit. Ang. Math. Mech.*, vol. **6**, pp. 291–294, 1926.

Keller, H. B., Numerical methods in boundary layer theory, *Ann. Rev. Fluid Mech.*, vol. **10**, pp. 417–433, 1978.

Rees, D. A. S., and Pop, I., Local thermal nonequilibrium in porous medium convection, In D. B. Ingham and I. Pop, Editors, *Transport Phenomena in Porous Media III*, Oxford: Pergamon, pp. 147–173, 2005.

Rees, D. A. S., Bassom, A. P., and Siddheshwar, P. G., Local thermal non-equilibrium effects arising from the injection of a hot fluid into a porous medium, *J. Fluid Mech.*, vol. **594**, pp. 379–398, 2008.

Rees, D. A. S., Microscopic modelling of the two-temperature model for conduction in heterogeneous media: Three-dimensional media, *Proc. of the 4$^{\mathrm{th}}$ Int. Conf. on Applications of Porous Media, Istanbul, Turkey,* 2009.

Rees, D. A. S., Microscopic modelling of the two-temperature model for conduction in heterogeneous media, *J. Porous Media*, vol. **13**, Paper 15, pp. 125–143, 2010.

Schumann, T. E. W., Heat transfer: A liquid flowing through a porous prism, *J. Franklin Institute*, vol. **208**, pp. 405–416, 1929.

Shook, G. M., Predicting thermal breakthrough in heterogeneous media from tracer tests, *Geothermics*, vol. **30**, pp. 573–589, 2001.

Stopa, J. and Wojnarowski, P., Analytical model of cold water front movement in a geothermal reservoir, *Geothermics*, vol. **35**, pp. 59–69, 2006.